Journal of Engineering Physics and Thermophysics, Vol. 79, No. 1, 2006

FREE CONVECTIVE HEAT EXCHANGE

CONJUGATE HEAT TRANSFER IN A CLOSED DOMAIN WITH A LOCALLY LUMPED HEAT-RELEASE SOURCE

G. V. Kuznetsov[a] **and M. A. Sheremet**[b]

UDC 669.86:536.21

Free convective heat transfer in a solution domain quite accurately modeling the cross section of the object of heat consumption has been investigated numerically. Typical velocity and temperature fields have been presented.

Introduction. Heat and energy saving is one current topical problem. Its solution is a fairly difficult and complex task. The complexity lies in the fact that one must generally not only model the process in question but also make an attempt at proposing variants of solution of the problem of heat and energy saving based on the investigation performed. An empirical analysis of technological heat-supply systems provides only stationary data on the object in question and makes it impossible to evaluate the dynamics of the process. Therefore, mathematical modeling of a combination of processes in actual systems consuming thermal energy is the most efficient means of solving such problems.

The transfer of heat in actual heat-supply objects is mainly by the mechanisms of heat conduction and free convection [1–3], with the convection processes being dominant. However, an important feature of the problem in question is a fundamentally conjugate, in essence, character of the heat exchange [4]. The thermal regime of any heat-supply object is determined not only by the intensity of the processes of heat transfer inside the object but also by the intensity of heat removal at its external boundaries. Furthermore, the heat-release source in actual systems is generally locally lumped, and problems in such a formulation significantly differ from most traditional problems of free convection [1–3]. Evaluations of the heat loss on typical objects are important in analyzing the processes of heat and energy supply. Such evaluations are also of independent importance.

The present work seeks to solve the problem of nonstationary conjugate heat transfer in a closed domain with a locally lumped heat-release source and inhomogeneous boundary conditions at both the external and internal boundaries.

Mathematical Model. We consider a boundary-value problem of heat transfer with allowance for conduction and natural convection for the domain presented in Fig. 1.

The solution domain represents a set of rectangles characterized by different dimensions and different thermophysical characteristics. Boundary conditions of the third kind which also allow for the radiative heat exchange with the environment are specified at one boundary, whereas heat-insulation conditions are specified at the other three boundaries. The domain is subdivided into subdomains with different thermophysical characteristics corresponding to the enclosing structures of the object of heat consumption and this object's cavity protected against cooling. A locally lumped heat-release source (battery) is to be found at the boundary between two subdomains.

The heat-consumption-object model investigated in this work (Fig. 1) fairly well describes a typical cross section of a room which passes through the heat-release source. In such a formulation, the process of transfer of heat in the typical heat-supply object analyzed is described by a system of nonstationary Navier–Stokes equations for the gas phase and a heat-conduction equation for the solid phase with nonlinear boundary conditions. Nonstationary two-di-

[a]Tomsk Polytechnic University, 30 Lenin Ave., Tomsk, 634050, Russia; [b]Tomsk State University, 36 Lenin Ave., Tomsk, 634050, Russia; email: Michael-sher@yandex.ru. Translated from Inzhenerno-Fizicheskii Zhurnal, Vol. 79, No. 1, pp. 56–63, January–February, 2006. Original article submitted December 15, 2004.

1062-0125/06/7901-0057

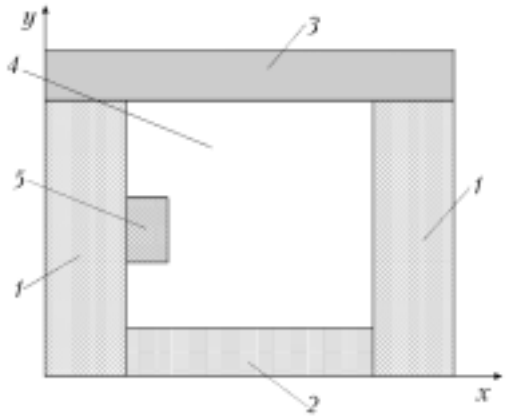

Fig. 1. Domain of solution of the problem in question: 1) brick; 2) wood; 3) concrete; 4) air; 5) locally lumped heat-release source.

mensional convection equations in the Boussinesq approximation [1–3] have been used to determine the flow and temperature fields in the gas phase. The length of the considered solution domain along the x axis was selected as the distance scale, and the time scale was selected to be 24 h, since this time interval is determining for the closed object [5, 6]. Dimensionless variables were introduced in the form $X = \frac{x}{L}$, $Y = \frac{y}{L}$, $\tau = \frac{t}{\tilde{t}}$, $U = \frac{u}{\tilde{V}}$, $V = \frac{v}{\tilde{V}}$, and $\Theta = \frac{T - T_0}{T_{\text{bat}} - T_0}$. Thus, the dimensionless Boussinesq equations in the velocity vortex-stream function–temperature variables can be written as follows:

$$\frac{1}{\text{Sh}}\frac{\partial \omega}{\partial \tau} + U\frac{\partial \omega}{\partial X} + V\frac{\partial \omega}{\partial Y} = \frac{1}{\text{Re}}\Delta\omega + \frac{\text{Gr}}{2\text{Re}^2}\frac{\partial \Theta}{\partial X}, \tag{1}$$

$$\Delta\psi = -2\omega, \tag{2}$$

$$\frac{1}{\text{Sh}}\frac{\partial \Theta}{\partial \tau} + U\frac{\partial \Theta}{\partial X} + V\frac{\partial \Theta}{\partial Y} = \frac{1}{\text{Re}\,\text{Pr}}\Delta\Theta; \tag{3}$$

for the gas phase in the domain in question (Fig. 1), and

$$\frac{\partial \Theta_i}{\partial \text{Fo}_i} = \Delta\Theta_i, \quad i = 1, 2, 3, \tag{4}$$

where $i = 1$ corresponds to brick, $i = 2$ to wood, and $i = 3$ to concrete, for the solid phase.

Dimensionless boundary conditions for system (1)–(4) have the form

$$\omega(0, Y, \tau) = 0, \quad \psi(0, Y, \tau) = 0, \quad \frac{\partial \Theta(0, Y, \tau)}{\partial X} = \text{Bi}\,\Theta(0, Y, \tau) + \text{Bi}\,\frac{T_0 - T_\text{e}}{T_{\text{bat}} - T_0} + Q, \quad X = 0,$$

$$Q = N\left[\left(\Theta(0, Y, \tau) + \frac{T_0}{T_{\text{bat}} - T_0}\right)^4 - \left(\frac{T_\text{e}}{T_{\text{bat}} - T_0}\right)^4\right],$$

at the remaining external boundaries, the conditions for the velocity vortex and the stream function are analogous, whereas for the temperature they are

$$\frac{\partial \Theta_i (X, Y, \tau)}{\partial X^k} = 0 , \quad X^1 \equiv X , \quad X^2 \equiv Y , \quad i = \overline{1, 3} ,$$

at the internal boundaries which are in parallel to the $0x$ axis, we have

$$\psi (X, \tilde{Y}, \tau) = 0 , \quad \frac{\partial \psi (X, \tilde{Y}, \tau)}{\partial Y} = 0 , \quad \Theta_i (X, \tilde{Y}, \tau) = \Theta_j (X, \tilde{Y}, \tau) ,$$

$$\frac{\partial \Theta_i (X, \tilde{Y}, \tau)}{\partial Y} = \lambda_{ji} \frac{\partial \Theta_j (X, \tilde{Y}, \tau)}{\partial Y} , \quad i = 2, 3 , \quad j = 1, 4 ;$$

at the internal boundaries which are in parallel to the $0y$ axis, we have

$$\psi (\tilde{X}, Y, \tau) = 0 , \quad \frac{\partial \psi (\tilde{X}, Y, \tau)}{\partial X} = 0 ,$$

$$\Theta_1 (\tilde{X}, Y, \tau) = \Theta_i (\tilde{X}, Y, \tau) , \quad \frac{\partial \Theta_1 (\tilde{X}, Y, \tau)}{\partial X} = \lambda_{i1} \frac{\partial \Theta_i (\tilde{X}, Y, \tau)}{\partial X} , \quad i = 2, 4 ;$$

on all the portions of the solution domain where the conjugation of materials with different thermophysical parameters occurs, we have

$$\Theta_i (X, Y, \tau) = \Theta_j (X, Y, \tau) , \quad \frac{\partial \Theta_i (X, Y, \tau)}{\partial X^k} = \lambda_{ji} \frac{\partial \Theta_j (X, Y, \tau)}{\partial X^k} , \quad i, j = \overline{1, 4} , \quad i \neq j , \quad k = 1, 2 .$$

The heat-release source was assumed to have a temperature constant over the entire period, and the boundary condition of the first kind $\Theta(X, Y, \tau) = 1$ was assumed to be fulfilled at its boundary. The values of the velocity vortex were computed from the Woods formula [7, 8]. At the initial instant of time, we had $\omega(X, Y, 0) = \psi(X, Y, 0) = 0$ and $\Theta(X, Y, 0) = 0$.

Solution of the Problem. Problem (1)–(4) with the corresponding boundary and initial conditions has been solved by the finite-difference method with the use of the basic techniques from [7–11]. Equations (1)–(4) were solved successively; each time step began with computation of the temperature field in both the gas phase and the solid phase (Eqs. (3) and (4)); thereafter, the Poisson equation for the stream function (2) was solved. Next we determined the boundary conditions for the velocity vector and solved Eq. (1). The Poisson equation was solved by the establishment method [10, 12].

To numerically solve Eqs. (1) and (2) we used the difference scheme constructed by analogy with the well-known scheme of variable directions [7, 13, 14] for solution of the heat-conduction equation. In this scheme, solution of a two-dimensional system is reduced to successive solution of one-dimensional systems, whereas solution of a one-dimensional system is reduced to successive solution of systems of difference equations with tridiagonal matrices.

The energy equation (3) was solved with the use of a locally one-dimensional scheme; approximation of convective terms was considered as being averaged relative to U and $|U|$ (or V and $|V|$) for the scheme to be independent of the sign of the velocity [7, 15].

To test the algorithms we solved two classical problems based on Navier–Stokes equations: flow of a liquid in a cavern with a moving boundary [7, 8, 16–18] and thermal gravitational convection on a square domain [7].

In solving both the test problems and the primal problem in the stationary regime, we checked the fulfillment of the integral balances of heat and mass flow rate:

$$\tilde{q}_{w1} = \tilde{q}_{w2} , \quad \int_0^1 u dy = 0 , \quad \int_0^1 v dx = 0 ,$$

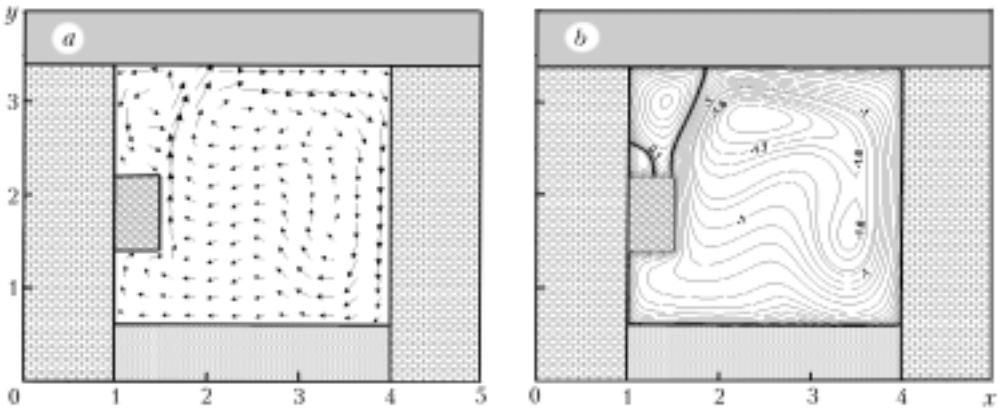

Fig. 2. Typical velocity field (a) and streamlines (b) for Sh = 1, Re = 20.7, Gr = 10^7, and Pr = 0.71. x, y, m.

where

$$\tilde{q}_{\mathrm{w}} = \int_0^1 q_{\mathrm{w}}(y)\, dy\,, \quad \left(q_{\mathrm{w}} = -\lambda_{\mathrm{w}} \left(\frac{\partial T}{\partial x} \right)_{\mathrm{w}} \right).$$

Calculation Results. Numerical investigations have been carried out for the following values of: the dimensionless numbers Sh = 1, Re = 20.7, Gr = 10^7, and Pr = 0.71; the governing temperatures T_{e} = 258 K, T_{bat} = 333 K, and T_0 = 293 K, and the dimensions of the solution domain L = 5 m and H = 4 m.

Figure 2 gives typical results of solution of the formulated boundary-value problems in the form of the velocity field $\mathbf{V}(x, y)$. It is clear from the figure that the heat-release source is responsible for the formation of four circulatory flows. Two vortices are located at the center of the air gap and represent circulatory air motion; the flow rises in the vicinity of the heat-release source, since the density of the warm air is lower than that of the cold air, and descends at the opposite cold wall. It is noteworthy that these central vortices are a result of the action of the lift on the air motion and represent the degeneration of a unified central vortex which takes a complex structure and disintegrates as the Gr number increases. Two more vortices are to be found above the heat-release source in the air gap of the solution domain in question, which are attributed to the position and finiteness of the dimensions of the heat-release source itself. The small vortex above the heat-release source represents the zone of secondary circulatory flow. No circulatory flows are observed below the source, which is attributable to the intensification of transfer processes above the source.

The temperature distribution clearly demonstrates the influence of the lift $g\beta(T_{\mathrm{bat}} - T_0)$ which appears due to the inhomogeneity of the temperature field [1–3].

Figure 3 shows that the temperature in the gas phase is distributed quite nonuniformly because of the influence of the buoyancy force. As is clear from the figure, the intensification of the process of heat transfer is maximum in the region of the upper corner of the heat-release source, where we have the joining of two vortices which subsequently cause the temperature field to be redistributed. The isotherm corresponding to 305 K becomes more extended toward the main central vortex and in so doing reaches its center. The circulatory flow in the central region closer to the boundary y = 0.6 m is responsible for the occurrence of local maxima (corresponding to 300 and 295 K) of the isotherms. Also, the heat-release source exerts an influence on the uniform temperature distribution on the rectangular portion at which it is located. The reason is that, in the formulation in question, the material was assumed to be isotropic in this subdomain.

We numerically analyzed the level of heat loss for the plane case of free convection and for one-dimensional cases of conductive heat transfer in the following regimes: (1) T_0 = 290 K and T_{bat} = 328 K, (2) T_0 = 293 K and T_{bat} = 333 K, and (3) T_0 = 298 K and 343 K. The heat fluxes from the room to the environment were calculated from the formula $q = \alpha(T_{\mathrm{m.w}} - T_{\mathrm{e}})$. We solved the problems of heat transfer due to the conduction regime in a one-dimensional formulation for the domains presented in Fig. 4. We considered the following boundary-value problem:

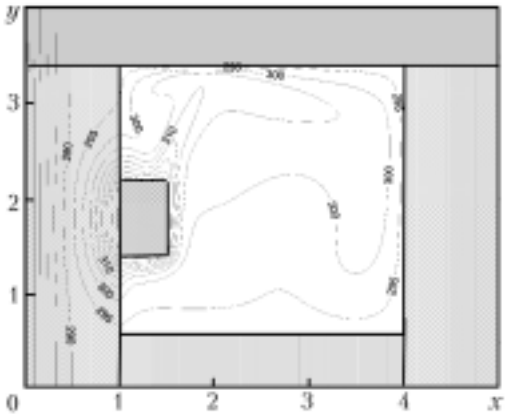

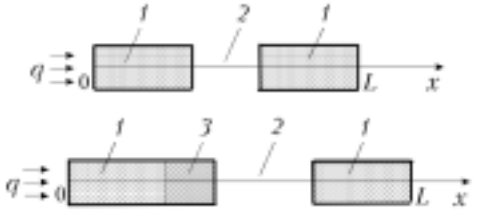

Fig. 3. Typical field of the temperature T for Sh = 1, Re = 20.7, Gr = 10^7, and Pr = 0.71. T, K; x, y, m.

Fig. 4. Domains of solution of the problem in question: 1) brick; 2) air; 3) locally lumped heat-release source.

$$\frac{\partial \Theta_i}{\partial \mathrm{Fo}_i} = \Delta \Theta_i , \quad i = 1, 2 , \tag{5}$$

where i = 1 corresponds to brick and i = 2 corresponds to air.

Dimensionless boundary conditions for system (5) have the form

$$\left. \frac{\partial \Theta (X, \tau)}{\partial X} \right|_{X=0} = \mathrm{Bi}\, \Theta (0, \tau) + \mathrm{Bi}\, \frac{T_0 - T_\mathrm{e}}{T_\mathrm{bat} - T_0} + Q , \quad X = 0 ,$$

where

$$Q = N \left[\left(\Theta (0, \tau) + \frac{T_0}{T_\mathrm{bat} - T_0} \right)^4 - \left(\frac{T_\mathrm{e}}{T_\mathrm{bat} - T_0} \right)^4 \right],$$

at the other external boundary, the condition for the temperature is

$$\left. \frac{\partial \Theta_1 (X, \tau)}{\partial X} \right|_{X=1} = 0 ,$$

on all remaining portions of the solution domain, where the conjugation of materials with different thermophysical parameters occurs, we have

$$\Theta_1 (X, \tau) = \Theta_2 (X, \tau) , \quad \frac{\partial \Theta_1 (X, \tau)}{\partial X} = \lambda_{21} \frac{\partial \Theta_2 (X, \tau)}{\partial X} .$$

The heat-release source was assumed to have a temperature constant over the entire period and the boundary condition of the first kind $\Theta(X, Y, \tau) = 1$ was assumed to be fulfilled at its boundary. At the initial instant of time, we had $\Theta(X, Y, 0) = 0$ (see Table 1).

An analysis of the calculated heat loss shows that, after 24 h, the outflow of heat from the solution domain to the environment at T_0 = 17°C and T_bat = 55°C is nearly 20% smaller than that at T_0 = 25°C and T_bat = 70°C. In the case of the one-dimensional model, we obtain somewhat understated values of the heat fluxes.

TABLE 1. Heat Loss for the Regimes in Question: (I), Plane Free Convection, (II), One-Dimensional Heat Conduction with a Heat-Release Source, (III), One-Dimensional Heat Conduction without a Heat-Release Source

T_0, K	T_{bat}, K	q, W/m^2		
		I	II	III
290	328	59.07	56.04	55.59
293	333	64.60	61.27	60.80
298	343	73.82	70.01	69.48

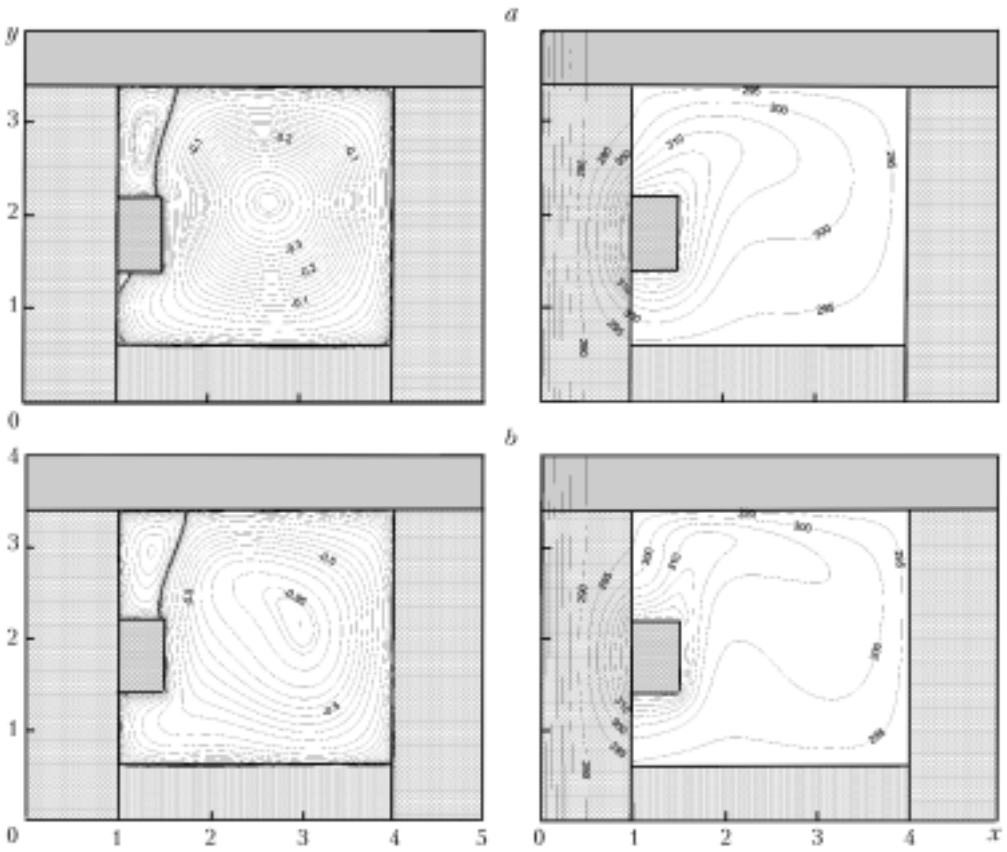

Fig. 5. Typical streamlines and field of the temperature T for Sh = 1, Re = 20.7, Pr = 0.71: Gr = 10^5 (a) and Gr = 10^6 (b). T, K; x, y, m.

This result illustrates the scales of a possible heat and energy saving in the case of the optimum values of the object's temperatures.

Also, we compared the temperature fields and the streamlines for different values of Gr = 10^5–10^6. The results are presented in Fig. 5.

Four circulatory flows are formed in the air gap for Gr = 10^5 (Fig. 5a). The largest vortex is at the center of the air gap and represents air motion on a spiral path. In the air gap of the solution domain in question, there are three more vortices: one vortex is above the heat-release source and the other two are below the source. It is noteworthy that the two vortices below the source represent one larger vortex disintegrated in this domain. The temperature in the air gap changes nonuniformly as well. The influence of the lift which causes the isotherms to extend toward the upper part of the solution domain in question is clearly seen in Fig. 5. Due to the circulatory motion of the air masses, the isotherm corresponding to 305 K bends toward the motion. As the Gr number increases 10 times (Fig. 5b), the structure of the central vortex changes and its center shifts toward the right-hand rectangular part of the solution domain; the air circulates elliptically, not in a circle. The vortices located earlier below the heat-release source decrease and are to be found in the corner domains, thus representing the circulation zones of the air masses. The

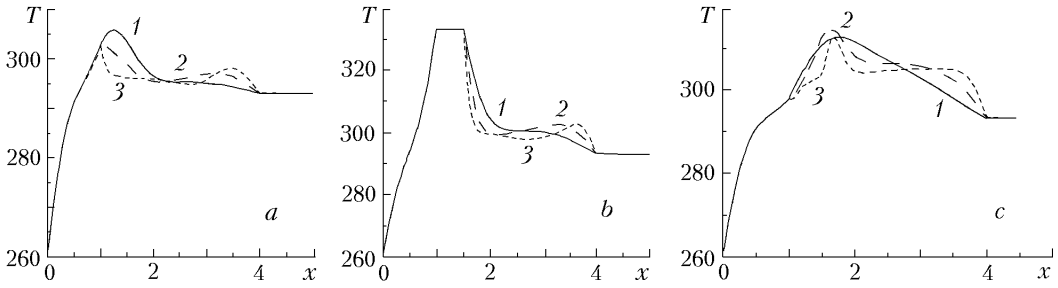

Fig. 6. Temperature distributions in the cross sections below the heat-release source y = 1.0 m (a), in the heat-release source y = 1.8 m (b), and above the heat-release source y = 2.8 (c) in different regimes (1) Gr = 10^5; 2) 10^6; 3) 10^7). T, K; x, m.

position of the maximum of the isotherms (Fig. 5b) shifts toward the upper part of the solution domain, and the constant-temperature curves themselves qualitatively reflect the motion of the air masses.

Figure 6a gives the temperature profiles in the cross section below the heat-release source for different values of the Gr number. It is seen that an increase of two orders of magnitude in Gr leads to a reduction of 9 K in the temperature directly below the heat-release source. Such a temperature distribution is attributed to the location of the cross section in the domain in question, since the vortex below the heat-release source degenerates with increase in Gr, which certainly cannot but reflect on the temperature distribution.

Figure 6b shows that the temperature near the heat-release source decreases with growth in the Gr number, since an intense transfer of warm air masses to the upper parts of the gap occurs. An increase in the temperature at the rectangular part of the solution domain (this part is opposite to the heat-release source) is seen.

An increase in the Gr number in the cross section above the heat-release zone (Fig. 6c) leads to a significant temperature redistribution, which is influenced by both the vortex above the heat-release source and the main vortex. As Gr increases 100 times, the temperature in the air gap on a segment of 1.7 m to 2.3 m decreases by 6 K, whereas in the region 3 m $< x <$ 4 m, the maximum temperature difference in these two regimes is equal to 6 K.

Conclusions. We have numerically investigated the regime of conjugate convective-conductive heat transfer in a rectangular domain with intense heat removal at one boundary and a local heat-release source. The results obtained characterize not only the temperature fields of a typical object of heat supply in the heat-transfer regime under study but can also provide an additional basis for construction and testing of models for analysis of the heat loss on heat-supply objects and mathematical modeling of the processes of force convection within the framework of the conjugate formulation.

Based on the numerical investigations carried out, we can infer that free convective flows in heat-supply objects typical in configuration are of great interest, which is attributed to the different types of behavior of the isotherms in the domain in question. As the Gr number increases, we have a structural change in the central vortex which is of primary importance in formation of the temperature profile in a room. Also, the vortex below the heat-release source degenerates with growth in Gr, which leads to a reduction in the temperature in this domain.

An analysis of the heat loss has shown that the plane model allows more accurate results than the one-dimensional model. The relative disagreement amounts to about 6%.

NOTATION

a, thermal diffusivity, m^2/sec; $Bi = \alpha L/\lambda_w$, Biot number; $Fo_i = a_i\tilde{t}/L^2$, Fourier number corresponding to the ith material; g, free-fall acceleration, m/sec^2; $Gr = \beta g_y L^3(T_{bat} - T_0)/\nu^2$, Grashof number; g_y, component of the acceleration of gravity in the projection onto the y axis (g_x = 0), m/sec^2; H, height of the solution domain in question along the y axis, m; L, length of the solution domain in question along the x axis, m; $N = \varepsilon\sigma L(T_{bat} - T_0)^3/\lambda_w$, number characterizing the ratio of the heat fluxes by radiation to the heat fluxes by conduction; $Pr = \nu/a$, Prandtl number; Q, dimensionless heat flux determining the role of conduction and radiation; q_w, heat flux at a point, W/m^2; $\tilde{q}_w$, heat flux through the boundary, W/m^2; $\tilde{q}_{w1}$, heat flux through the boundary x = 0, W/m^2; $\tilde{q}_{w2}$, heat flux from the heat-release

source, W/m^2; Re = $\tilde{V}L/\nu$, Reynolds number; Sh = $\tilde{V}\tilde{t}/L$, Strouhal number; T, temperature, K; T_e, environmental temperature, K; T_0, initial temperature of the solution domain, K; T_{bat}, temperature on the heat-release source, K; $T_{m.w}$, mean temperature on the exterior wall $x = 0$; t, time, sec; $\tilde{t}$, time scale, sec; U and V, dimensionless velocity components corresponding to u and v; $\tilde{V}$, velocity scale, m/sec; u and v, velocity components in the projection onto the x and y axes, respectively, m/sec; X, Y, dimensionless coordinates corresponding to x and y; $\tilde{X}$ and $\tilde{Y}$, dimensionless coordinates along the X and Y axes, which correspond to one internal boundary of the air gap; X^k, kth unit vector of the coordinate system; x, y, Cartesian coordinates; α, heat-exchange coefficient, W/(m^2·K); β, temperature coefficient of volumetric expansion, K^{-1}; Δ, Laplace operator; ε, reduced emissivity factor; Θ, dimensionless temperature; Θ_i, dimensionless temperature of the ith material; λ_w, thermal conductivity of the wall, W/(m·K); $\lambda_{ij} = \lambda_i/\lambda_j$, relative thermal conductivity; λ_i, thermal conductivity of the ith material, W/(m·K); ν, coefficient of kinematic viscosity, m^2/sec; σ, Stefan–Boltzmann constant, W/(m^2·K^4); τ, dimensionless time; ψ, dimensionless stream function $U = \partial\psi/\partial Y$; $V = -\partial\psi/\partial X$, dimensionless analog of the vortex-velocity vector. Subscripts and superscripts: 0, corresponds to the initial instant of time; e, environment; bat, heat-release source; w, wall; m.w, mean on the wall; i and j, material No.; k, ordinal No. of the unit vector of the coordinate system.

REFERENCES

1. Y. Jaluria, *Natural Convection Heat and Mass Transfer* [Russian translation], Mir, Moscow (1983).
2. Yu. A. Sokovishin and O. G. Martynenko, *Introduction to the Theory of Free-Convective Heat Transfer* [in Russian], Izd. LGU, Leningrad (1982).
3. B. Gebhart, Y. Jaluria, R. L. Mahajan, and B. Sammakia, *Buoyancy-Induced Flows and Transport* [Russian translation], Vol. 1, Mir, Moscow (1991).
4. A. V. Luikov, A. A. Aleksashenko, and V. A. Aleksashenko, *Conjugate Problems of Convective Heat Transfer* [in Russian], Nauka i Tekhnika, Minsk (1971).
5. V. V. Ivanov, L. V. Karaseva, and S. A. Tikhomirov, Modeling of heat-transfer processes in multilayered protecting structures, in: *Proc. III Russian National Conf. on Heat Transfer* [in Russian], Vol. 7 (2002), pp. 131–134.
6. D. V. Matyukhov, M. I. Nizovtsev, V. I. Terekhov, and V. V. Terekhov, Determination of heat-protection characteristics of thermal-inertial structures under the conditions of nonstationary heat transfer, in: *Proc. III Russian National Conf. on Heat Transfer* [in Russian], Vol. 7 (2002), pp. 184–187.
7. V. M. Paskonov, V. I. Polezhaev, and L. A. Chudov, *Numerical Simulation of Heat- and Mass-Transfer Processes* [in Russian], Nauka, Moscow (1984).
8. P. J. Roache, *Computational Fluid Dynamics* [Russian translation], Mir, Moscow (1980).
9. A. A. Samarskii, *The Theory of Difference Schemes* [in Russian], Nauka, Moscow (1977).
10. N. N. Kalitkin, *Numerical Methods* [in Russian], Nauka, Moscow (1978).
11. I. S. Berezin and N. P. Zhidkov, *Computational Methods* [in Russian], Vol. 2, Fizmatgiz, Moscow (1962).
12. V. M. Verzhbitskii, *Principles of Numerical Methods* [in Russian], Vysshaya Shkola, Moscow (2002).
13. J. Douglas, On the numerical integration of $u_{xx} + u_{yy} = u_t$ by implicit methods, *J. Soc. Industr. Appl. Math.*, **3**, No. 1, 42–65 (1955).
14. D. W. Peaceman and H. H. Rachford, The numerical solution of parabolic and elliptic differential equations, *J. Soc. Industr. Appl. Math.*, **3**, No. 1, 28–41 (1955).
15. A. A. Samarskii and P. N. Vabishchevich, *Numerical Methods for Solving Convection-Diffusion Problems* [in Russian], Éditorial URSS, Moscow (2003).
16. C. A. J. Fletcher, *Computational Techniques for Fluid Dynamics* [Russian translation], Vol. 2, Mir, Moscow (1991).
17. S. E. Rogers and D. Kwak, An upwind differencing scheme for the incompressible Navier–Stokes equations, *Appl. Numer. Math.*, **8**, 43–64 (1991).
18. U. Ghia, K. N. Ghia, and C. T. Shin, High-Re solutions for incompressible flow using the Navier–Stokes equations and a multigrid method, *J. Comput. Phys.*, **48**, 387 (1982).